A DS-CDMA System Using Despreading Sequences Weighted by Adjustable Chip Waveforms

Yuejin Huang, *Member, IEEE,* and Tung-Sang Ng, *Senior Member, IEEE*

***Abstract*— This paper evaluates the performance of a direct-sequence code-division multiple-access system using coherent receivers in which the despreading sequences are weighted by adjustable chip waveforms. The chip weighting waveforms under consideration are designed for multiple-access interference (MAI) rejection. Assuming that the received chip waveforms are rectangular, new expressions for the signal-to-interference-plus-noise ratio (SINR) of the decision variable are derived when different weighted despreading sequences (WDS's) are used in the receiver. The novelty of the derived expressions is that each of the expressions, when the system parameters are given, is determined only by one parameter of the adjustable chip waveforms employed. As a result, we can simply tune the parameter to its optimal value in real-time for MAI rejection without knowing the other users' spreading codes, timing, and phase. The criterion for tuning the parameter is to maximize the SINR of the decision variable based on the relative strength between the additive Gaussian white noise and the MAI. Numerical results show that when the multiple-access interference is significant, the receivers using WDS's outperform significantly the conventional receiver using a rectangular despreading sequence. Brief analysis for band-limited spreading signals is also provided to reveal the practical implications of the proposed technique.**

***Index Terms*—Adjustable chip waveform, DS-CDMA, multiple-access interference, noise whitening.**

I. Introduction

In A direct-sequence code-division multiple-access (DS-CDMA) system with perfect power control, the major limitation in performance, and hence capacity, is due to multipath fading and multiple-access interference (MAI). It is generally accepted that some form of diversity is required in the system to cope with multipath fading. For MAI, its effect on performance cannot be reduced by simply increasing the received signal-to-background-noise power ratio due to the requirement of power control in a DS-CDMA system. As a result, the receiver error rate tends to level out to a constant value, or floor, depending on the system parameters. With the objective of MAI rejection, an optimum multiuser receiver was proposed in [1]. However, it is extremely complex. Subsequently, a number of suboptimal receivers using simplified structures have been proposed [2]–[6], [16]. These suboptimal multiuser receivers require locking and despreading some or all of the co-user signals, hence they are still too complex to be implemented in practice.

Based on a noise whitening approach, a simple structure called the integral equation receiver was proposed in [7]. The integral equation receiver employs a despreading function, which is the solution of a Fredholm integral equation of the second kind. The resulting despreading function consists of $2N^2$ exponential terms with the number of coefficients proportional to N^2, where N is the processing gain. However, in a typical situation, it is still not easy to find the optimum despreading function in a practical implementation when N is relatively large. We note that the despreading function given in [7] emphasizes the transitions in the received signal from the desired user for MAI rejection. This leads us to consider weighting the despreading sequence by simple adjustable chip waveforms which are determined by only one parameter. The resulting weighted despreading sequence (WDS) is easy to tune to achieve the best performance.

In this paper, we analyze the performance of a DS-CDMA system using coherent receivers with the proposed WDS's and show how the system signal-to-interference-plus-noise ratio (SINR) is improved by tuning the parameter of the chip weighting waveforms. These receivers are equivalent to specific matched filters with impulse responses matched to the WDS's. The performance of the proposed receiver is marginally poorer than that of the integral equation receiver (see Fig. 7). However, the proposed receivers can be implemented with much less complexity.

The organization of the paper is as follows. In Section II, the system model is described. In Section III, the SINR of the decision variable for a DS-CDMA system is derived under the proposed WDS's. This is followed by numerical results in Section IV. A discussion on issues of practical significance, band-limited spreading signals, and implementation of the proposed system is given in Section V, and finally, in Section VI, conclusions are given.

II. System Model

Suppose there are K CDMA users accessing the channel. User k transmits a binary data signal $b_k(t)$ and employs a spreading signal $a_k(t)$ to spread each data bit. The spreading and data signals for the kth user are given by $a_k(t) =$

Paper approved by U. Mitra, the Editor for Spread Spectrum/Equalization of the IEEE Communications Society. Manuscript received January 23, 1997; revised August 13, 1997, June 30, 1998, and May 8, 1999. This work was supported by the Hong Kong Research Grants Council and by the CRCG of The University of Hong Kong.

Y. Huang was with the Department of Electrical and Electronic Engineering, The University of Hong Kong, Hong Kong. He is now with the Department of Electrical and Computer Engineering, McGill University, Montreal, P.Q. H3A-247, Canada.

T.-S. Ng is with the Department of Electrical and Electronic Engineering, The University of Hong Kong, Hong Kong (e-mail: tsng@eee.hku.hk).

Publisher Item Identifier S 0090-6778(99)09777-9.

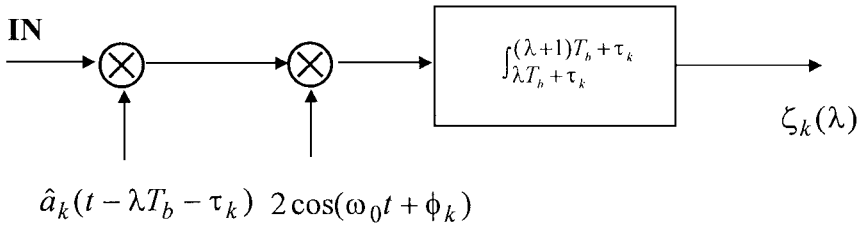

Fig. 1. The structure of a coherent receiver with a WDS for the kth user.

$\sum_{j=-\infty}^{\infty} a_j^{(k)} P_{T_c}(t-jT_c)$ and $b_k(t)=\sum_{j=-\infty}^{\infty} b_j^{(k)} P_{T_b}(t-jT_b)$, where T_c and T_b are the chip and data durations, respectively, and $P_x(y)=1$, for $0<y<x$, and $P_x(y)=0$ otherwise. In our study, both sequences $b_j^{(k)}$ and $a_j^{(k)}$ are modeled as independent random variables taking values -1 or $+1$ with equal probabilities. It is assumed that there are N chips of a spreading signal in the interval of each data bit T_b ($T_b=NT_c$), and the spreading signal has a period that is much longer than N. The transmitted signal for the kth user is

$$S_k(t)=\sqrt{2P}b_k(t)a_k(t)\cos(\omega_0 t+\theta_k) \tag{1}$$

where the transmitted power P and the carrier frequency ω_0 are common to all users. Thus, the received signal $r(t)$ at the base station can be represented as

$$\begin{aligned} r(t) &= \sum_{k=1}^{k} S_k(t-\tau_k)+n(t) \\ &= \sqrt{2P}\sum_{k=1}^{K} b_k(t-\tau_k)a_k(t-\tau_k)\cos(\omega_0 t+\phi_k)+n(t) \end{aligned} \tag{2}$$

where K denotes the number of active users. The random time delays and phases along the communication links between the K transmitters and the receiver are denoted by τ_k and ϕ_k $(=\theta_k-\omega_0\tau_k)$, for $1\le k\le K$, respectively. The ambient channel noise $n(t)$ is modeled as an additive white Gaussian noise (AWGN) process with two-sided spectral density $N_0/2$. The random variables $\{\tau_k\}$ and $\{\phi_k\}$ are independent of one another and uniformly distributed on $[0,T_b]$ and $[0,2\pi]$, respectively.

For binary phase-shift keying modulation, the structure of a coherent receiver with WDS's for the kth user is shown in Fig. 1, where $\zeta_k(\lambda)$ is the decision variable and $\hat{a}_k(t)$ is the WDS which will be described in detail below.

III. System Performance

A. WDS's

In a DS-CDMA system, the MAI is the sum of many independent co-user signals and we can model the MAI as a zero-mean, colored, Gaussian process. By means of the central limit theorem, the accuracy of the Gaussian assumption should increase as the processing gain N and number of users K increase. Gaussian approximations have been used in the study of similar models (e.g., [8]–[10]) and have been reported to be accurate even for a moderate number of co-users. If the signals of co-users are shifted in time by a random amount distributed uniformly between 0 and T_c, the MAI becomes a statistically stationary random process [11]. A CDMA receiver for the kth user transmitting in stationary, colored, Gaussian noise was derived in [7] with the objective of suppressing MAI. The receiver was termed the integral equation receiver as the desired despreading function $q(t)$ was the solution of the following integral equation:

$$\int_0^{T_b} C_n(t-\tau)q(t)\,d\tau=-N_0q(t)+a_k(t),\qquad 0\le t\le T_b \tag{3}$$

where $C_n(\tau)$ is the autocorrelation function of the MAI. Equation (3) is a Fredholm integral equation of the second kind. As pointed out in [12], the integral equation receiver is equivalent to a generalized matched filter for the colored noise case. The despreading sequence obtained from the solution of (3) maximizes the SINR. If the MAI is a Gaussian process, maximizing the SINR is equivalent to minimizing the probability of error in a CDMA system. The integral (3) has been solved in [7] for the case in which the spreading pulses are rectangular. The resulting despreading function $q(t)$ consists of $2N^2$ exponential terms, with the number of coefficients proportional to N^2. When the spreading codes have a period much larger than N, (3) needs to be solved for every symbol period for as many symbol periods as there exist within one period of the spreading code. Clearly, because of considerable processing requirements, it is not easy to obtain and implement the optimum despreading function $q(t)$ in practice when N is large or the spreading code period is much larger than N.

To overcome this issue, we propose a WDS for the kth receiver as follows:

$$\hat{a}_k(t)=\sum_{j=-\infty}^{\infty} a_j^{(k)} w_j^{(k)}\left(t-jT_c \,\middle|\, \left\{c_j^{(k)},c_{j+1}^{(k)}\right\}\right) \tag{4}$$

where $c_j^{(k)}=a_{j-1}^{(k)}a_j^{(k)}$, and $w_j^{(k)}(t\mid\{c_j^{(k)},c_{j+1}^{(k)}\})$, for $0\le t\le T_c$, is the jth chip weighting waveform for the kth receiver, conditioned on the status of three consecutive chips $\{c_j^{(k)},c_{j+1}^{(k)}\}=\{a_{j-1}^{(k)}a_j^{(k)},a_j^{(k)}a_{j+1}^{(k)}\}$. Each $c_j^{(k)}$ is a random variable which indicates whether or not the next element of the kth spreading signal is the same as the preceding element. $c_j^{(k)}=-1$ implies $a_{j-1}^{(k)}\ne a_j^{(k)}$, and a transition occurs between the two consecutive chips, while $c_j^{(k)}=1$ implies $a_{j-1}^{(k)}=a_j^{(k)}$, and no transition occurs between the two consecutive chips. Because $\{a_j^{(k)}:0\le j\le N-1\}$ is a set of independent and identically distributed random variables taking values $+1$ or -1 with equal probabilities, $\{c_j^{(k)}:0\le j\le N-1\}=\{c_j^{(k)}\}_{j=0}^{N-1}$ is a set of independent

and identically distributed random variables taking values $+1$ or -1 with equal probabilities. In our analysis, we define the jth chip conditional weighting waveform for the kth receiver as

$$w_j^{(k)}\left(t \,\middle|\, \left\{c_j^{(k)}, c_{j+1}^{(k)}\right\}\right) = \begin{cases} m_1(t), & \text{if } c_j^{(k)} = +1 \quad \text{and} \quad c_{j+1}^{(k)} = +1 \\ m_2(t), & \text{if } c_j^{(k)} = -1 \quad \text{and} \quad c_{j+1}^{(k)} = -1 \\ m_3(t), & \text{if } c_j^{(k)} = -1 \quad \text{and} \quad c_{j+1}^{(k)} = +1 \\ m_4(t), & \text{if } c_j^{(k)} = +1 \quad \text{and} \quad c_{j+1}^{(k)} = -1 \end{cases} \tag{5}$$

where $m_p(t)$ for $p \in [1,2,3,4]$ are the proposed chip weighting waveforms which will be described in detail below. Noting that the despreading functions shown in [7, Fig. 5] emphasize the transitions of the received signal from the desired user, we now define the elements of the chip weighting waveform vector $\{m_1(t), m_2(t), m_3(t), m_4(t)\}$ for the following two cases: 1) exponential chip waveforms (EW); 2) stepping chip waveforms (SW). For the EW case, the chip weighting waveforms $m_p(t)$ for $p = 1, 2, 3$, and 4, denoted by $m_p^{(e)}(t)$, are defined as

$$\begin{aligned} m_1^{(e)}(t) &= e^{-\gamma/2} P_{T_c}(t) \\ m_2^{(e)}(t) &= e^{-\gamma t/T_c} P_{T_c/2}(t) + e^{-\gamma(1-t/T_c)} P_{T_c/2}(t - T_c/2) \\ m_3^{(e)}(t) &= e^{-\gamma t/T_c} P_{T_c/2}(t) + e^{-\gamma/2} P_{T_c/2}(t - T_c/2) \\ m_4^{(e)}(t) &= e^{-\gamma/2} P_{T_c/2}(t) + e^{-\gamma(1-t/T_c)} P_{T_c/2}(t - T_c/2) \end{aligned} \tag{6}$$

where $\gamma \in [0, \infty)$ is a parameter of the exponential chip weighting waveforms. Similarly, for the SW case, the chip weighting waveforms $m_p(t)$ for $p = 1, 2, 3$, and 4, denoted by $m_p^{(s)}(t)$, are defined as

$$\begin{aligned} m_1^{(s)}(t) &= L(\varepsilon) P_{T_c}(t) \\ m_2^{(s)}(t) &= P_{T_c}(t) - [1 - L(\varepsilon)] P_{T_c - 2T_\Delta}(t - T_\Delta) \\ m_3^{(s)}(t) &= P_{T_\Delta}(t) + L(\varepsilon) P_{T_c - T_\Delta}(t - T_\Delta) \\ m_4^{(s)}(t) &= L(\varepsilon) P_{T_c - T_\Delta}(t) + P_{T_c}(t) - P_{T_c - T_\Delta}(t) \end{aligned} \tag{7}$$

where $T_\Delta \in (0, T_c/2]$, $\varepsilon = T_c/T_\Delta \in [2, \infty)$ is a parameter of the stepping chip weighting waveforms, and $L(\varepsilon) \in [0, 1]$ is a monotonically decreasing function of ε. For ease of implementation, we simply define $L(\varepsilon) = [C(\varepsilon/2 - 1) + 1]^{-1}$ where the constant C is chosen equal to 10 (see Section IV for how this value was chosen) in what follows. When $\gamma = 0$ in (6) and $\varepsilon = 2$ in (7), the chip waveforms $m_p^{(e)}(t)$ and $m_p^{(s)}(t)$, for all $p \in \{1, 2, 3, 4\}$, reduce to the rectangular pulse $P_{T_c}(t)$. For the two cases, Fig. 2 shows diagrams of the chip weighting waveforms, and Fig. 3 shows waveforms of length-14 segments of a spreading signal and the corresponding WDS's.

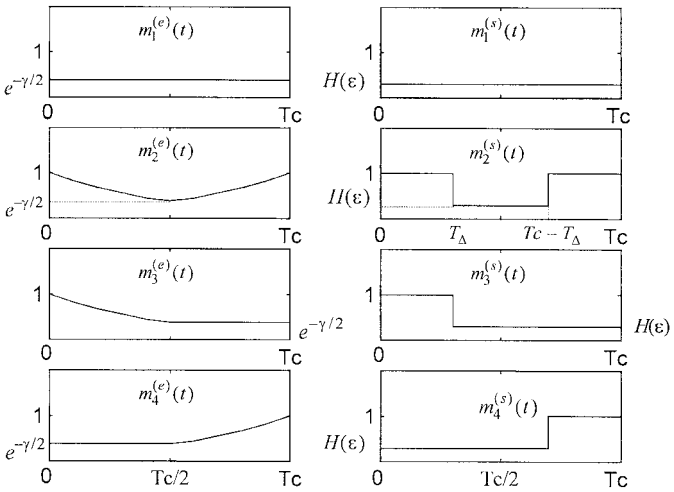

Fig. 2. The chip weighting waveforms: (a) EW and (b) SW.

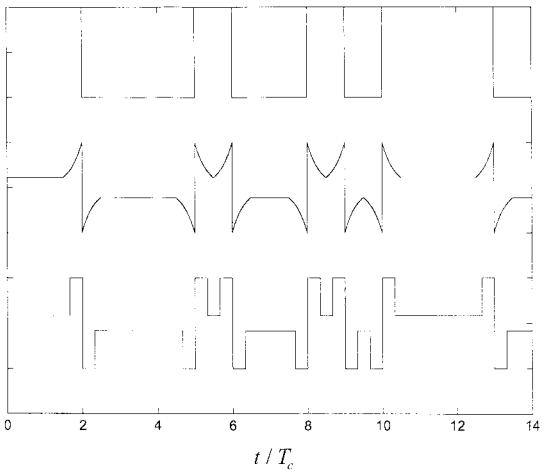

Fig. 3. Waveforms for a length-14 segment of a spreading sequence and the corresponding WDS's: (a) spreading sequence, (b) WDS for the EW case, and (c) WDS for the SW case.

B. Performance Analysis

We arbitrarily choose the ith user as the desired user and analyze the performance of the proposed receiver for data symbol $b_\lambda^{(i)}$. For coherent demodulation, the conditional output random variable of the ith user receiver, denoted by $\zeta_i(\lambda)$, which is equivalent to a specific matched filter output with the impulse response matched to $2\hat{a}_i(t)\cos(\omega_0 t) P_{T_b}(t)$, can be expressed as

$$\zeta_i(\lambda) = \int_{\lambda T_b + \tau_i}^{(\lambda+1)T_b + \tau_i} \{2r(t)\hat{a}_i(t - \lambda T_b - \tau_i)\cos(\omega_0 t + \phi_i)\}\, dt \tag{8}$$

where $\cos(\omega_0 t + \phi_i)$ is the coherent carrier reference and $\hat{a}_i(t - \lambda T_b - \tau_i)$ is the WDS of the reference user. Since the carrier frequency f_0 is much larger than T_b^{-1} in a practical system, the double-frequency terms in (8) can be ignored, and (8) reduces to

$$\zeta_i(\lambda) = S_i\left(\lambda \,\middle|\, \left\{c_j^{(i)}\right\}_{j=0}^{N-1}\right) + N_i\left(\lambda \,\middle|\, \left\{c_j^{(i)}\right\}_{j=0}^{N-1}\right) + \sum_{k=1(k\neq 1)}^{K} Y_{\{c_j^{(i)}\}}^{(k,i)} \tag{9}$$

where the first, second, and third components, respectively, are the conditional desired signal, the noise, and the MAI components, which are described in detail below. From (8), the conditional desired signal term $S_i(\lambda \mid \{c_j^{(i)}\}_{j=0}^{N-1})$ in (9),

conditioned on the set $\{c_j^{(i)}\}_{j=0}^{N-1}$, can be expressed as

$$\begin{aligned} S_i\left(\lambda \,\middle|\, \left\{c_j^{(i)}\right\}_{j=0}^{N-1}\right) &= \sqrt{2P}\int_{\lambda T_b+\tau_i}^{(\lambda+1)T_b+\tau_i} b_\lambda^{(i)} a_i(t-\tau_i)\hat{a}_i(t-\lambda T_b-\tau_i)\,dt \\ &= \sqrt{2P} b_\lambda^{(i)} \sum_{j=0}^{N-1}\int_{jT_c}^{(j+1)T_c} w_j^{(i)}\left(t-jT_c \,\middle|\, \left\{c_j^{(i)}, c_{j+1}^{i}\right\}\right) dt. \end{aligned} \tag{10}$$

From (4)–(7), we obtain (11), shown at the bottom of the page. Thus, making a change of the integral limits in (10) and then using (11), $S_i(\lambda \mid \{c_j^{(i)}\}_{j=0}^{N-1})$ can be written as

$$S_i\left(\lambda \,\middle|\, \left\{c_j^{(i)}\right\}_{j=0}^{N-1}\right) = b_\lambda^{(i)}\sqrt{2P} \left[2\hat{N}_i\int_0^{T_c/2} m_2(t)\,dt + (N-\hat{N}_i)\int_0^{T_c} m_1(t)\,dt\right] \tag{12}$$

where $\hat{N}_i$ is a random variable which represents the number of occurrences of $c_j^{(i)} = -1$ for all $j \in [0, N-1]$. Note that $S_i(\lambda \mid \{c_j^{(i)}\}_{j=0}^{N-1})$ in (12) is conditioned on $\hat{N}_i$. However, to simplify the notation, we still use $S_i(\lambda \mid \{c_j^{(i)}\}_{j=0}^{N-1})$ in (12) instead of $S_i(\lambda \mid \hat{N}_i)$ because $\hat{N}_i$ depends on $\{c_j^{(i)}\}_{j=0}^{N-1}$. From (8), the additive Gaussian noise term $N_i(\lambda \mid \{c_j^{(i)}\}_{j=0}^{N-1})$ in (9) can be expressed as

$$N_i\left(\lambda \,\middle|\, \left\{c_j^{(i)}\right\}_{j=0}^{N-1}\right) = \int_0^{T_b} [n_c(t)\cos\phi_i - n_s(t)\sin\phi_i]\hat{a}_i(t)\,dt \tag{13}$$

where the terms $n_c(t)$ and $n_s(t)$ are the low-pass equivalent components of the noise $n(t)$. Using an approach similar to that which led to (12), the conditional variance of the noise term $N_i(\lambda \mid \{c_j^{(i)}\}_{j=0}^{N-1})$, conditioned on $\{c_j^{(i)}\}_{j=0}^{N-1}$ and denoted by $\sigma^2_{N|\{c_j^{(i)}\}}$, is therefore given by

$$\sigma^2_{N|\{c_j^{(i)}\}} = N_0\left[2\hat{N}_i\int_0^{T_c/2}[m_2(t)]^2\,dt + (N-\hat{N}_i)\int_0^{T_c}[m_1(t)]^2\,dt\right]. \tag{14}$$

Also from (8), the third term in (9) that is the MAI term for the ith receiver, denoted by $I_{k,i}$, is given by

$$\begin{aligned} I_{k,i} &= \sum_{k=1(k\neq i)}^{K} Y^{(k,i)}_{\{c_j^{(i)}\}} \\ &= \sqrt{2P}\sum_{k=1(k\neq i)}^{K}\cos(\phi_i-\phi_k)\left[b_{\lambda-1}^{(k)}R_{ik}(\tau_{ki}) + b_\lambda^{(k)}\hat{R}_{ik}(\tau_{ki})\right] \end{aligned} \tag{15}$$

where $\tau_{ki} = \tau_k - \tau_i$, $R_{ik}(\tau) = \int_0^\tau a_k(t-\tau)\hat{a}_i(t)\,dt$, and $\hat{R}_{ik}(\tau) = \int_\tau^{T_b} a_k(t-\tau)\hat{a}_i(t)\,dt$. Since $Y^{(k,i)}_{\{c_j^{(i)}\}}$ are uncorrelated for different k, the conditional variance of the MAI term $I_{k,i}$, conditioned on $\{c_j^{(i)}\}_{j=0}^{N-1}$ and denoted by $\sigma^2_{I|\{c_j^{(i)}\}}$, is then given by

$$\begin{aligned} \sigma^2_{I|\{c_j^{(i)}\}} &= E\left[I_{k,i}^2 \,\middle|\, \left\{c_j^{(i)}\right\}_{j=0}^{N-1}\right] \\ &= P\sum_{\substack{k=1\\k\neq i}}^{k} E\Big[R_{ik}^2(\tau_{ki}) + \hat{R}_{ik}^2(\tau_{ki}) \\ &\qquad + 2b_{\lambda-1}^{(k)}b_\lambda^{(k)}R_{ik}(\tau_{ki})\hat{R}_{ik}(\tau_{ki}) \,\Big|\, \left\{c_j^{(i)}\right\}_{j=0}^{N-1}\Big] \end{aligned} \tag{16}$$

where $E[\cdot \mid \{c_j^{(i)}\}_{j=0}^{N-1}]$ denotes the ensemble average with respect to all the random variables in $[\cdot]$, except $c_j^{(i)}$. Since $E[b_{\lambda-1}^{(k)}b_\lambda^{(k)}] = 0$, we have

$$\sigma^2_{I|\{c_j^{(i)}\}} = P\sum_{k=1,k\neq i}^{K}\left\{\bar{\Theta}_{\{c_j^{(i)}\}}(R_{ik},\hat{R}_{ik}) - \mu_{ik|\{c_j^{(i)}\}}\right\} \tag{17}$$

where $\bar{\Theta}_{\{c_j^{(i)}\}}(R_{ik},\hat{R}_{ik}) = E[\{R_{ik}(\tau_{ki})+\hat{R}_{ik}(\tau_{ki})\}^2 \,|\, \{c_j^{(i)}\}_{j=0}^{N-1}]$ and $\mu_{ik|\{c_j^{(i)}\}} = 2E[R_{ik}(\tau_{ki})\hat{R}_{ik}(\tau_{ki})\,|\,\{c_j^{(i)}\}_{j=0}^{N-1}]$. Both $\bar{\Theta}_{\{c_j^{(i)}\}}(R_{ik},\hat{R}_{ik})$ and $\mu_{ik|\{c_j^{(i)}\}}$ are conditioned on $\{c_j^{(i)}\}_{j=0}^{N-1}$. Let $\tau_{ki} = mT_c - \tau_0$, for $m \in [1, N]$, where τ_0 is a random variable distributed uniformly between 0 and T_c. We obtain

$$\begin{aligned} &R_{ik}(\tau_{ki}) + \hat{R}_{ik}(\tau_{ki}) \\ &\qquad = \sum_{j=0}^{N-1} a_{N-m+j}^{(k)} a_j^{(i)} f\left(\tau_0 \,\middle|\, \left\{c_{j-1}^{(i)}, c_j^{(i)}, c_{j+1}^{(i)}\right\}\right) \end{aligned} \tag{18}$$

where

$$\begin{aligned} &f\left(\tau_0 \,\middle|\, \left\{c_{j-1}^{(i)}, c_j^{(i)}, c_{j+1}^{(i)}\right\}\right) \\ &\qquad = c_j^{(i)}\int_{T_c-\tau_0}^{T_c} w_{j-1}^{(i)}\left(t \,\middle|\, \left\{c_{j-1}^{(i)}, c_j^{(i)}\right\}\right) dt \\ &\qquad\quad + \int_0^{T_c-\tau_0} w_j^{(i)}\left(t \,\middle|\, \left\{c_j^{(i)}, c_{j+1}^{(i)}\right\}\right) dt. \end{aligned} \tag{19}$$

Since $E[a_{j1}^{(k)}a_{j2}^{(k)}] = 0$, for $j1 \neq j2$, and $E[R_{ik}(\tau_{ki}) + \hat{R}_{ik}(\tau_{ki})] = 0$, we obtain (20), shown at the bottom of the next page, where $\Gamma^{(i)}_{\{\upsilon_1,\upsilon_2,\upsilon_3\}}$ is the number of occurrences of $\{c_{j-1}^{(i)}, c_j^{(i)}, c_{j+1}^{(i)}\} = \{\upsilon_1,\upsilon_2,\upsilon_3\}$, for all $j \in [0, N-1]$ in the ith WDS. Each element of $\{\upsilon_1,\upsilon_2,\upsilon_3\}$ takes the value $+1$ or -1 with equal probability. It is clear that $\Sigma_{\{\upsilon_1,\upsilon_2,\upsilon_3\}}\Gamma^{(i)}_{\{\upsilon_1,\upsilon_2,\upsilon_3\}} = N$. Substituting (5) into (20) leads to (21), shown at the bottom of the next page. According to

$$\int_{jT_c-T_c/2}^{jT_c+T_c/2} w_j^{(i)}\left(t-jT_c \,\middle|\, \left\{c_j^{(i)}, c_{j+1}^{i}\right\}\right) dt = \begin{cases} 2\displaystyle\int_0^{T_c/2} m_2(t)\,dt \quad \text{or} \quad 2\int_{T_c/2}^{T_c} m_4(t)\,dt, & \text{if } c_{j+1}^{(i)} = -1 \\ \displaystyle\int_0^{T_c} m_1(t)\,dt \quad \text{or} \quad 2\int_{T_c/2}^{T_c} m_3(t)\,dt, & \text{if } c_{j+1}^{(i)} = +1. \end{cases} \tag{11}$$

Appendix A, the term $\mu_{ik|\{c_j^{(i)}\}}$ in (17) is given by

$$\mu_{ik|\{c_j^{(i)}\}} = 2E\left[c_0^{(i)} \int_0^{\tau_0} w_0^{(i)}\left(t \mid \left\{c_0^{(i)}, c_1^{(i)}\right\}\right) dt \cdot \int_{\tau_0}^{T_c} w_{N-1}^{(i)}\left(t \mid \left\{c_{N-1}^{(i)}, c_0^{(i)}\right\}\right) dt\right] \quad (22)$$

and then we obtain

$$\left|\mu_{ik|\{c_j^{(i)}\}}\right| \le 2E\left[\int_0^{\tau_0} m_2(t)\,dt \int_{\tau_0}^{T_c} m_2(t)\,dt\right] \le E\left[\int_0^{T_c} m_2(t)\,dt\right]^2. \quad (23)$$

Note that there are N terms in (21) and $|\mu_{ik|\{c_j^{(i)}\}}| \le [\int_0^{T_c} m_2(t)\,dt]^2$. Assuming that N is large, the effect of $E_{\{c_j^{(i)}\}}[\mu_{ik|\{c_j^{(i)}\}}]$ on $E_{\{c_j^{(i)}\}}\lfloor \bar{\Theta}_{\{c_j^{(i)}\}}(R_{ik}, \hat{R}_{ik})\rfloor$ in (17) is negligible (see Section III-C for justification) where $E_{\{c_j^{(i)}\}}[\cdot]$ denotes the ensemble average over all $c_j^{(i)}$, for $-\infty < j < +\infty$, and over all other random variables in $[\cdot]$. We therefore ignore the term $\mu_{ik|\{c_j^{(i)}\}}$ in (17) in the analysis. Thus, the conditional variance of the MAI term is approximately given by

$$\sigma^2_{I|\{c_j^{(i)}\}} \approx P(K-1)\bar{\Theta}_{\{c_j^{(i)}\}}(R_{ik}, \hat{R}_{ik}) \quad (24)$$

where the term $\bar{\Theta}_{\{c_j^{(i)}\}}(R_{ik}, \hat{R}_{ik})$ is given by (21). The conditional variances of the MAI term for both the EW and SW cases, denoted by $\sigma^2_{IE|\{c_j^{(i)}\}}$ and $\sigma^2_{IS|\{c_j^{(i)}\}}$, are given by (B-1) and (B-3) in Appendix B, respectively.

Thus, by definition, the SINR of the decision variable, conditioned on $\{c_j^{(i)}\}_{j=0}^{N-1}$, can be expressed as

$$\mathrm{SINR_i} = \left\{ \frac{\sigma^2_{\mathrm{N}|\{\mathrm{c_j^{(i)}}\}}}{\left[\mathrm{S}\left(\lambda \mid \left\{\mathrm{c_j^{(i)}}\right\}_{\mathrm{j=0}}^{\mathrm{N-1}}\right)\right]^2} + \frac{\sigma^2_{\mathrm{I}|\{\mathrm{c_j^{(i)}}\}}}{\left[\mathrm{S}\left(\lambda \mid \left\{\mathrm{c_j^{(i)}}\right\}_{\mathrm{j=0}}^{\mathrm{N-1}}\right)\right]^2} \right\}^{-1} \quad (25)$$

where $S(\lambda \mid \{c_j^{(i)}\}_{j=0}^{N-1})$, $\sigma^2_{N|\{c_j^{(i)}\}}$, and $\sigma^2_{I|\{c_j^{(i)}\}}$ are expressed by (12), (14), and (24), respectively. Substituting (6) into (12) and (14) and then apply the resulting expressions as well as (B-1) into (25), the SINR for the EW case, conditioned on $\{c_j^{(i)}\}_{j=0}^{N-1}$ and denoted by $\mathrm{SINR_r^{(e)}}$, is given by

$$\mathrm{SINR_i^{(e)}} = \left\{ \frac{\gamma[\chi(1-\mathrm{e}^{-\gamma}) + \gamma(1-\chi)\mathrm{e}^{-\gamma}]}{2\bar{\gamma}_b[2\chi(1-\mathrm{e}^{-\gamma/2}) + \gamma(1-\chi)\mathrm{e}^{-\gamma/2}]^2} + \frac{(K-1)\Xi^{(e)}\left(\Gamma^{\{c_j^{(i)}\}}, \gamma\right)}{2N[2\chi(e^{\gamma/2}-1) + \gamma(1-\chi)]^2} \right\}^{-1} \quad (26)$$

where $E_b = PT_b$, $\bar{\gamma}_b = E_b/N_0$, $\chi = \hat{N}_i/N$, and $\Xi^{(e)}(\Gamma^{\{c_j^{(i)}\}}, \gamma)$ is given by (B-2). Similarly, substituting (7) into (12) and (14), and then substituting the resulting expressions of both (12) and (14) as well as (B-3) into (25),

$$\begin{aligned}
\bar{\Theta}_{\{c_j^{(i)}\}}(R_{ik}, \hat{R}_{ik}) &= \sum_{j=0}^{N-1} E\left[f^2\left(\tau_0 \mid \left\{c_{j-1}^{(i)}, c_j^{(i)}, c_{j+1}^{(i)}\right\}\right)\right] \\
&= \Gamma^{(i)}_{\{-1,-1,-1\}} E[f^2(\tau_0 \mid \{-1,-1,-1\})] + \Gamma^{(i)}_{\{-1,-1,1\}} E[f^2(\tau_0 \mid \{-1,-1,1\})] \\
&\quad + \Gamma^{(i)}_{\{-1,1,-1\}} E[f^2(\tau_0 \mid \{-1,1,-1\})] + \Gamma^{(i)}_{\{-1,1,1\}} E[f^2(\tau_0 \mid \{-1,1,1\})] \\
&\quad + \Gamma^{(i)}_{\{1,1,-1\}} E[f^2(\tau_0 \mid \{1,1,-1\})] + \Gamma^{(i)}_{\{1,-1,-1\}} E[f^2(\tau_0 \mid \{1,-1,-1\})] \\
&\quad + \Gamma^{(i)}_{\{1,-1,1\}} E[f^2(\tau_0 \mid \{1,-1,1\})] + \Gamma^{(i)}_{\{1,1,1\}} E[f^2(\tau_0 \mid \{1,1,1\})]
\end{aligned} \quad (20)$$

$$\begin{aligned}
&\bar{\Theta}_{\{c_j^{(i)}\}}(R_{ik}, \hat{R}_{ik}) \\
&= \Gamma^{(i)}_{\{-1,-1,-1\}} E\left[-\int_{T_c-\tau_0}^{T_c} m_2(t)\,dt + \int_0^{T_c-\tau_0} m_2(t)\,dt\right]^2 + \Gamma^{(i)}_{\{-1,-1,1\}} E\left[-\int_{T_c-\tau_0}^{T_c} m_2(t)\,dt + \int_0^{T_c-\tau_0} m_3(t)\,dt\right]^2 \\
&\quad + \Gamma^{(i)}_{\{-1,1,-1\}} E\left[\int_{T_c-\tau_0}^{T_c} m_3(t)\,dt + \int_0^{T_c-\tau_0} m_4(t)\,dt\right]^2 + \Gamma^{(i)}_{\{-1,1,1\}} E\left[\int_{T_c-\tau_0}^{T_c} m_3(t)\,dt + \int_0^{T_c-\tau_0} m_1(t)\,dt\right]^2 \\
&\quad + \Gamma^{(i)}_{\{1,-1,-1\}} E\left[-\int_{T_c-\tau_0}^{T_c} m_4(t)\,dt + \int_0^{T_c-\tau_0} m_2(t)\,dt\right]^2 + \Gamma^{(i)}_{\{1,-1,1\}} E\left[-\int_{T_c-\tau_0}^{T_c} m_4(t)\,dt + \int_0^{T_c-\tau_0} m_3(t)\,dt\right]^2 \\
&\quad + \Gamma^{(i)}_{\{1,1,-1\}} E\left[\int_{T_c-\tau_0}^{T_c} m_1(t)\,dt + \int_0^{T_c-\tau_0} m_4(t)\,dt\right]^2 + \Gamma^{(i)}_{\{1,1,1\}} E\left[\int_0^{T_c} m_1(t)\,dt\right]^2
\end{aligned} \quad (21)$$

the SINR for the SW case, conditioned on $\{c_j^{(i)}\}_{j=0}^{N-1}$ and denoted by $\mathrm{SINR}_{\mathbf{i}}^{(\mathrm{s})}$, is given by

$$\mathrm{SINR}_{\mathbf{i}}^{(\mathrm{s})} = \left\{ \frac{\varepsilon[2\chi + (\varepsilon - 2\chi)\mathrm{H}^2(\varepsilon)]}{2\bar{\gamma}_{\mathrm{b}}[2\chi + (\varepsilon - 2\chi)\mathrm{H}(\varepsilon)]^2} + \frac{(K-1)\Xi^{(s)}\left(\Gamma^{\{c_j^{(i)}\}}, \varepsilon\right)}{2\varepsilon N[2\chi + (\varepsilon - 2\chi)H(\varepsilon)]^2} \right\}^{-1} \quad (27)$$

where $\Xi^{(s)}(\Gamma^{\{c_j^{(i)}\}}, \varepsilon)$ is given by (B-4). When $\gamma = 0$ in (26) and $\varepsilon = 2$ in (27), which correspond to employing rectangular despreading sequence in the reference receiver, the two previous expressions reduce to the same $\mathrm{SINR}_{\mathbf{i}}$, conditioned on $\hat{N}_i$, given by

$$\mathrm{SINR}_{\mathbf{i}} = \left(\frac{(\mathrm{K}-1)\varpi(\hat{\mathrm{N}}_{\mathrm{i}})}{3\mathrm{N}} + \frac{\mathrm{N}_0}{2\mathrm{E}_{\mathrm{b}}} \right)^{-1} \quad (28)$$

where $\varpi(\hat{N}_i) = 3/2 - \hat{N}_i/N$. Let $\hat{N}_i = N/2$ in (28), which is equivalent to replacing $\varpi(\hat{N}_i)$ by $E[\varpi(\hat{N}_i)]$ in (28). Then, (28) reduces to

$$\mathrm{SINR}_{\mathbf{i}} = \left(\frac{\mathrm{K}-1}{3\mathrm{N}} + \frac{\mathrm{N}_0}{2\mathrm{E}_{\mathrm{b}}} \right)^{-1}. \quad (29)$$

Comparing (29) with the SNR_i given by [13, eq. (17)], we see that the difference between the two equations is due to different definitions of the SINR.

Note that $\mathrm{SINR}_{\mathbf{i}}^{(\mathrm{e})}$ in (26) and $\mathrm{SINR}_{\mathbf{i}}^{(\mathrm{e})}$ in (27) are dependent on the spreading sequence $\{c_j^{(i)}\}_{j=0}^{N-1}$. Since it is assumed that all spreading sequences are random binary sequences, there should be relatively little difference between $\hat{N}_i$ and $E_{\{c_j^{(i)}\}}[\hat{N}_i]$, and also between $\Gamma_{\{\upsilon_1,\upsilon_2,\upsilon_3\}}^{(i)}$ and $E_{\{c_j^{(i)}\}}[\Gamma_{\{\upsilon_1,\upsilon_2,\upsilon_3\}}^{(i)}]$ in the set of all possible sequences when N is large. To achieve a simple expression of the SINR for all code sequences, it is reasonable to define an average signal power to average 'noise' power ratio as

$$\overline{\overline{\mathrm{SINR}}} = \left(\frac{E_{\{c_j^{(i)}\}}\left[\sigma^2_{N|\{c_j^{(i)}\}}\right]}{E^2_{\{c_j^{(i)}\}}\left[S\left(\lambda \middle| \left\{c_j^{(i)}\right\}_{j=0}^{N-1}\right)\right]} + \frac{E_{\{c_j^{(i)}\}}\left[\sigma^2_{I|\{c_j^{(i)}\}}\right]}{E^2_{\{c_j^{(i)}\}}\left[S\left(\lambda \middle| \left\{c_j^{(i)}\right\}_{j=0}^{N-1}\right)\right]} \right)^{-1}. \quad (30)$$

Although the $\overline{\overline{\mathrm{SINR}}}$ defined in (30) is not exactly the $\mathrm{SINR}_{\mathbf{i}}$ given in (25) for a specific code sequence, it is a tradeoff between the SINR for all users when N is large. The larger the processing gain N, the smaller the relative error between $\overline{\overline{\mathrm{SINR}}}$ and $\mathrm{SINR}_{\mathbf{i}}$. Note that for the EW and SW cases, the $\overline{\overline{\mathrm{SINR}}}$ are represented by $\overline{\overline{\mathrm{SINR}}}_{(e)}$ and $\overline{\overline{\mathrm{SINR}}}_{(s)}$, respectively. Substituting (6) into (30) and noting that $E_{\{c_j^{(i)}\}}[\hat{N}_i] = N/2$ and $E_{\{c_j^{(i)}\}}[\Gamma_{\{\upsilon_1,\upsilon_2,\upsilon_3\}}^{(i)}] = N/8$ for any realization of $\{\upsilon_1, \upsilon_2, \upsilon_3\}$, we get

$$\overline{\overline{\mathrm{SINR}}}_{(e)} = \left\{ \frac{\gamma[1 + (\gamma-1)e^{-\gamma}]}{\bar{\gamma}_b[2 + (\gamma-2)e^{-\gamma/2}]^2} + \frac{2(K-1)\bar{\Xi}^{(e)}(\gamma)}{N[2(e^{\gamma/2}-1) + \gamma]^2} \right\}^{-1} \quad (31)$$

where

$$\bar{\Xi}^{(e)}(\gamma) = \left(\frac{1}{2} - \frac{\gamma}{2} + \frac{5\gamma^2}{12} + \frac{9}{2\gamma} + e^{\gamma/2} - \frac{6}{\gamma}e^{\gamma/2} + \frac{3}{2\gamma}e^{\gamma} \right). \quad (32)$$

Similarly, substituting (7) into (30), we obtain

$$\overline{\overline{\mathrm{SINR}}}_{(s)} = \left\{ \frac{\varepsilon[1 + (\varepsilon-1)L^2(\varepsilon)]}{2\bar{\gamma}_b[1 + (\varepsilon-1)L(\varepsilon)]^2} + \frac{(K-1)\bar{\Xi}^{(s)}(\varepsilon)}{2\varepsilon N[1 + (\varepsilon-1)L(\varepsilon)]^2} \right\}^{-1} \quad (33)$$

where

$$\bar{\Xi}^{(s)}(\varepsilon) = \left[\left(\frac{2\varepsilon^3}{3} - 2\varepsilon + 2 \right) L^2(\varepsilon) + (2\varepsilon - 3)L(\varepsilon) + 1 \right]. \quad (34)$$

The main utility of (31) and (33) would be in the rough determination of the value of the parameter (γ or ε) of the corresponding WDS, which maximizes the system SINR for each case.

C. Accuracy of the Conditional Variance of MAI

The conditional variances $\sigma^2_{IE|\{c_j^{(i)}\}}$ and $\sigma^2_{IS|\{c_j^{(i)}\}}$ for the EW and SW cases are derived using (24) with the assumption that $|\mu_{ik|\{c_j^{(i)}\}}|$ is much smaller than $\bar{\Theta}_{\{c_j^{(i)}\}}(R_{ik}, \hat{R}_{ik})$ in (17) when N is large. If the despreading sequence of interest consists of rectangular pulses, it is clear that the assumption is justified from (21) and (23). However, as the chip waveforms of the WDS's are no longer rectangular in the proposed system, it is important to evaluate the effect of $\mu_{ik|\{c_j^{(i)}\}}$ on $\bar{\Theta}_{\{c_j^{(i)}\}}(R_{ik}, \hat{R}_{ik})$. For this purpose, we consider an appropriate measure of the effect. This measure is the ratio of $|E_{\{c_j^{(i)}\}}[\mu_{ik|\{c_j^{(i)}\}}]|$ to $E_{\{c_j^{(i)}\}}[\bar{\Theta}_{\{c_j^{(i)}\}}(R_{ik}, \hat{R}_{ik})]$, denoted by ρ, and is given by

$$\rho = \frac{\left|E_{\{c_j^{(i)}\}}\left[\mu_{ik|\{c_j^{(i)}\}}\right]\right|}{E_{\{c_j^{(i)}\}}\left[\bar{\Theta}_{\{c_j^{(i)}\}}(R_{ik}, \hat{R}_{ik})\right]}. \quad (35)$$

For the EW and SW cases, we denote the ratio ρ by $\rho^{(e)}$ and $\rho^{(s)}$, respectively. Then, according to Appendix C, we obtain

$$\rho^{(e)} = \frac{|\Omega^{(e)}(\gamma)|}{N\bar{\Xi}^{(e)}(\gamma)} \quad \text{and} \quad \rho^{(s)} = \frac{|\Omega^{(s)}(\varepsilon)|}{N\bar{\Xi}^{(s)}(\varepsilon)} \quad (36)$$

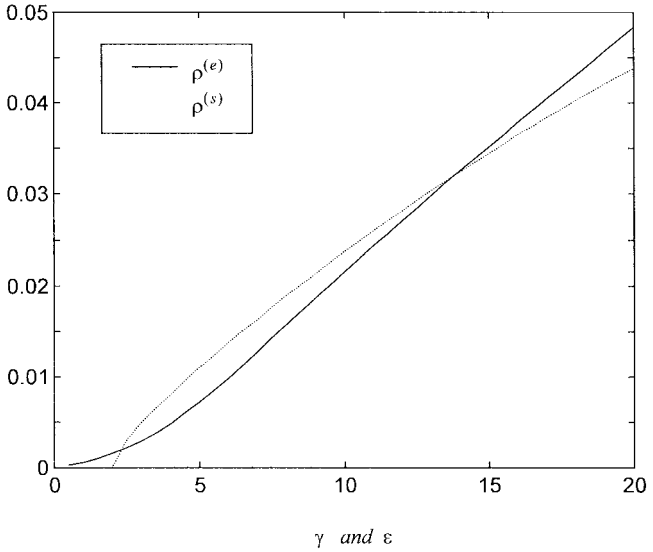

Fig. 4. The ratios of $|E_{\{c_j^{(i)}\}}[\mu_{ik|\{c_j^{(i)}\}}]|$ to $E_{\{c_j^{(i)}\}}[\bar{\Theta}_{\{c_j^{(i)}\}}(R_{ik}, \hat{R}_{ik})]$ for the EW and SW cases.

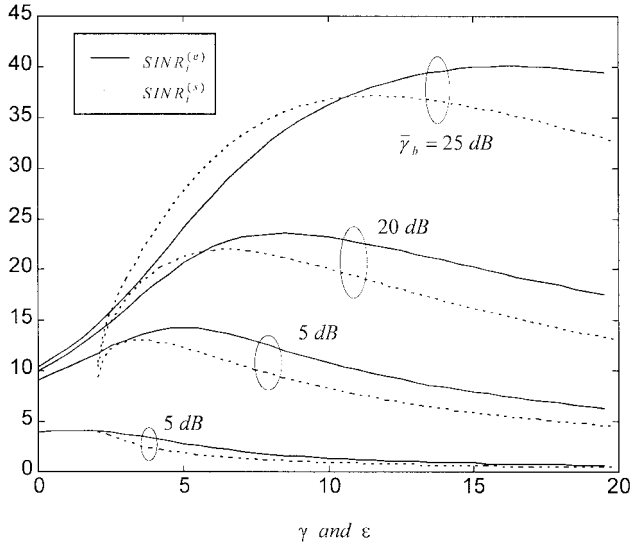

Fig. 5. $\mathrm{SINR_i}$ versus the parameters γ and ε for various values of $\bar{\gamma}_b$ when $N = 255$ and $K = 75$.

where

$$\Omega^{(e)}(\gamma) = -\frac{1}{2} + \frac{5}{2\gamma} - \frac{\gamma}{8} + \frac{7\gamma^2}{48} - \frac{\gamma e^{\gamma/2}}{8} + 2e^{\gamma/2} - \frac{4e^{\gamma/2}}{\gamma} + \frac{3e^{\gamma}}{2\gamma} - e^{\gamma}$$

$$\Omega^{(s)}(\varepsilon) = \left\{ L^2(\varepsilon)\left(\frac{7}{6} + \varepsilon^2 - \varepsilon\right) + L(\varepsilon)(3\varepsilon - 2 - \varepsilon^2) + \frac{5}{6} - \varepsilon \right\}. \quad (37)$$

In Fig. 4, we plot $\rho^{(e)}$ and $\rho^{(s)}$ versus the parameters γ and ε, when $N = 255$. The solid line represents $\rho^{(e)}$ and the dashed line represents $\rho^{(s)}$. It is clear that $\rho^{(e)} = 0$ at $\gamma = 0$ and $\rho^{(s)} = 0$ at $\varepsilon = 2$, which means that the average error of both (B-1) and (B-3) due to ignoring the term $\mu_{ik|\{c_j^{(i)}\}}$ is zero when the chip waveforms of the despreading sequence are rectangular pulses. Both curves in Fig. 4 show that the effect of $E_{\{c_j^{(i)}\}}[\mu_{ik|\{c_j^{(i)}\}}]$ on $E_{\{c_j^{(i)}\}}[\bar{\Theta}_{\{c_j^{(i)}\}}(R_{ik}, \hat{R}_{ik})]$ is negligible for moderate values of γ or ε. This suggests that (B-1) and (B-3) obtained in Appendix B are valid for relatively large N (say $N \geq 128$).

IV. Numerical Results

In this section, we present numerical results on the performance of the proposed coherent receivers in a DS-CDMA system. We demonstrate how the parameters (γ and ε) of the WDS's in both the EW and SW cases affect the $\mathrm{SINR_i}$ of the reference receiver for the data symbol $b_\lambda^{(i)}$ for a certain signal to background noise ratio $\bar{\gamma}_b = E_b/N_0$. We also show the bit-error-rate (BER) performance for each case. As the values of N and K used in this study are reasonably large, we can make the Gaussian assumption to evaluate the BER as an indication of the system performance. Since we have modeled the MAI as zero-mean Gaussian process, the probability of error P_e for the data symbol $b_\lambda^{(i)}$ in all the BER curves is defined as $P_e = Q(\sqrt{\max[\mathrm{SINR_i}]})$ where

$$Q(x) = (2\pi)^{-1/2} \int_x^\infty \exp(-t^2/2)\, dt \quad (38)$$

and $\max[\mathrm{SINR_i}]$ is the maximum value of $\mathrm{SINR_i}$. For the EW and SW cases, we replace $\mathrm{SINR_i}$ by $\mathrm{SINR_i^{(e)}}$ and $\mathrm{SINR_i^{(s)}}$ in the expression of P_e for the corresponding probabilities of error, denoted by $P_e^{(e)}$ and $P_e^{(s)}$, respectively. To minimize the probability of error, either γ or ε is tuned according to the value of $\bar{\gamma}_b$ to maximize the $\mathrm{SINR_i}$ for each case. When N is large, the average probability of error $\bar{\bar{P}}_e$ for the set of all possible sequences is defined as $P_e = Q(\sqrt{\max[\mathrm{SINR}]})$. Similarly, for the EW and SW cases, we replace $\overline{\overline{\mathrm{SINR}}}$ by $\overline{\overline{\mathrm{SINR}}}_{(e)}$ and $\overline{\overline{\mathrm{SINR}}}_{(s)}$ in the expression of $\bar{\bar{P}}_e$ for the corresponding probabilities of error, denoted by $\overline{\overline{P_e^{(e)}}}$ and $\overline{\overline{P_e^{(s)}}}$, respectively. In the following, it is assumed that the ith user's spreading sequence for the duration of data symbol $b_\lambda^{(i)}$ is a random binary sequence with length $N = 255$. In this sequence, $\hat{N}_i = 134$, $\Gamma^{(i)}_{\{-1,-1,-1\}} = 33$, $\Gamma^{(i)}_{\{-1,-1,1\}} + \Gamma^{(i)}_{\{1,-1,-1\}} = 70$, $\Gamma^{(i)}_{\{-1,1,1\}} + \Gamma^{(i)}_{\{1,1,-1\}} = 60$, $\Gamma^{(i)}_{\{-1,1,-1\}} = 36$, $\Gamma^{(i)}_{\{1,-1,1\}} = 31$, and $\Gamma^{(i)}_{\{1,1,1\}} = 25$. Because the period of the spreading code is much larger than N, the values of both the SINR and the BER for other symbols can be calculated simply based on other sets of $\{\Gamma^{(i)}_{\{\upsilon_1,\upsilon_2,\upsilon_3\}}\}$. Before computing any numerical results, the constant C in the expression of $L(\varepsilon)$ for the SW case needs to be chosen. By plotting $\mathrm{SINR_i^{(s)}}$'s against the parameter ε for various values of $\bar{\gamma}_b$ and C, we find $C = 10$ is a good compromise between the high and low values of $\bar{\gamma}_b$, and thus this value is chosen for this study.

In Fig. 5, $\mathrm{SINR_i^{(e)}}$ and $\mathrm{SINR_i^{(s)}}$ are plotted using the parameters γ and ε as the independent variables for various values of $\bar{\gamma}_b$ when $K = 75$. Note that the y-axis of Fig. 5 is not in decibels. It is clear that the WDS reduces to the rectangular spreading sequence when $\gamma = 0$ for the EW case or when $\varepsilon = 2$ for the SW case. Therefore, $\mathrm{SINR_i^{(e)}}$ at $\gamma = 0$ and $\mathrm{SINR_i^{(s)}}$

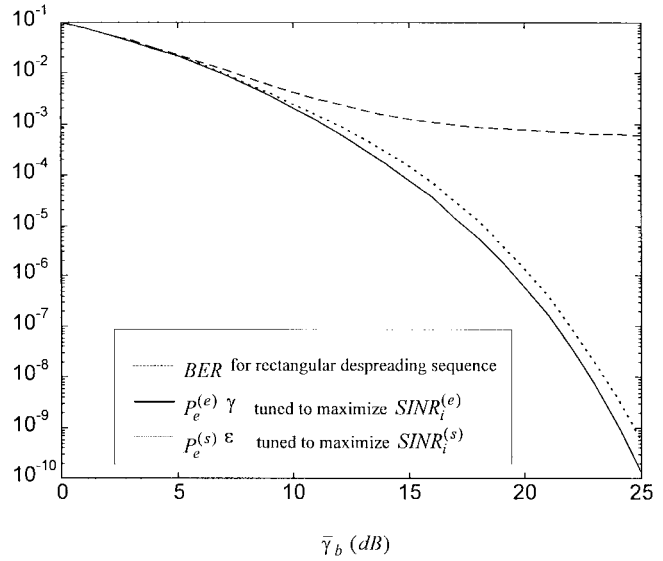

Fig. 6. BER versus $\bar{\gamma}_b$ for different WDS's when $N = 255$ and $K = 75$.

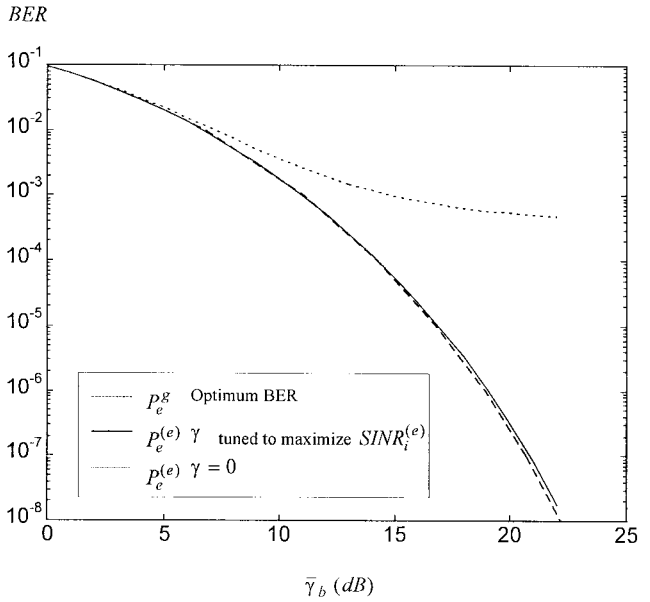

Fig. 7. Performance comparison between the integral equation receiver and the proposed receiver when $N = 31$ and $K = 9$.

at $\varepsilon = 2$ have the same value which corresponds to the $\mathrm{SINR_i}$ when the chip waveforms of the despreading sequence of the reference user are rectangular. These curves show that γ and ε should be tuned for different values of $\bar{\gamma}_b$ in order to maximize the $\mathrm{SINR_i^{(e)}}$ and $\mathrm{SINR_i^{(s)}}$, respectively. They also indicate that the WDS can be simply replaced by the rectangular spreading sequence with little loss of either $\mathrm{SINR_i^{(e)}}$ or $\mathrm{SINR_i^{(s)}}$ when the MAI is insignificant. For example, when $\bar{\gamma}_b \leq 5$ dB, either the $\mathrm{SINR_i^{(e)}}$ at $\gamma = 0$ or the $\mathrm{SINR_i^{(s)}}$ at $\varepsilon = 2$ is very close to the maximum value of the $\mathrm{SINR_i}$ in each case. This suggests that at low $\bar{\gamma}_b$, the proposed receiver reduces to conventional correlation receiver. On the other hand, when MAI dominates over AWGN, γ and ε should be tuned with respect to each $\bar{\gamma}_b$ to maximize the $\mathrm{SINR_i^{(e)}}$ and $\mathrm{SINR_i^{(s)}}$, respectively. For example, when $\bar{\gamma}_b = 20$ dB, the WDS with $\gamma \approx 8.5$ or $\varepsilon \approx 6.5$ can maximize the $\mathrm{SINR_i}$ for each case. It is also observed from Fig. 5 that the maximum value of $\mathrm{SINR_i^{(e)}}$ is always larger than that of $\mathrm{SINR_i^{(s)}}$ at the same value of $\bar{\gamma}_b$. This suggests that the despreading sequence weighted by the EW is preferable.

Fig. 6 shows the BER performance of the proposed receiver with different WDS's. The top curve (dashed line) is the BER for a conventional correlation receiver with a rectangular despreading sequence. This corresponds to the case that either $\gamma = 0$ or $\varepsilon = 2$ in the proposed WDS's. The two curves in the bottom correspond to the BER for the proposed receivers where γ and ε are tuned explicitly to each $\bar{\gamma}_b$ to maximize the $\mathrm{SINR_i^{(e)}}$ and $\mathrm{SINR_i^{(s)}}$. We can see from this figure that in low $\bar{\gamma}_b$ ($\leq$5 dB), where the BER's are mostly caused by AWGN, tuning γ or ε has little effect on the maximum value of the corresponding $\mathrm{SINR_i}$ so that the BER's do not differ much regardless of the WDS's. On the other hand, in relative high $\bar{\gamma}_b$ ($\geq$15 dB), the BER's are mostly caused by the MAI so that the BER's in this region can be reduced substantially by tuning either γ or ε. Fig. 6 also shows clearly that the receiver with each of the proposed WDS's performs substantially better than the conventional correlation receiver with rectangular despreading sequences.

For the purpose of comparison, Fig. 7 plots $P_e^{(i)}$ at $\gamma = 0$ (dotted line), $P_e^{(i)}$ where γ is tuned to maximize the $\mathrm{SINR_i^{(e)}}$ (solid line) and the optimum P_e^g shown in [7, Fig. 6] (dashed line) obtained by using the optimal despreading function that is the solution of the integral equation given by (3), all using the same sequence of length $N = 31$ when $K = 9$. The sequence employed is the first Gold code given in [7, Table I]. In this sequence, $\hat{N}_i = 16$, $\Gamma^{(i)}_{\{-1,-1,-1\}} = 4$, $\Gamma^{(i)}_{\{-1,-1,1\}} + \Gamma^{(i)}_{\{1,-1,-1\}} = 8$, $\Gamma^{(i)}_{\{-1,1,1\}} + \Gamma^{(i)}_{\{1,1,-1\}} = 8$, $\Gamma^{(i)}_{\{-1,1,-1\}} = 4$, $\Gamma^{(i)}_{\{1,-1,1\}} = 4$, and $\Gamma^{(i)}_{\{1,1,1\}} = 3$. From this figure, we can see that the performance of the proposed receiver with exponential WDS is almost identical to that of the integral equation receiver. Also for the purpose of comparison, the BER curves of the proposed receiver for the EW case are plotted in Fig. 8 by using different spreading codes in [7, Table I]. Note that for the first, fifth, and sixth codes from that table, which have the same elements of the set $\{\Gamma^{(i)}_{\{v_1,v_2,v_3\}}\}$, the BER performance is identical. In Fig. 8, the solid, dashed, dotted, dash-dot, and point curves correspond to the BER performance when the first, second, third, fourth, and seventh codes in the table are employed as the reference code, respectively.

In Fig. 9, the parameters γ_{opt} and $\varepsilon_{\mathrm{opt}}$ which maximize the $\mathrm{SINR_i^{(e)}}$ and $\mathrm{SINR_i^{(s)}}$, respectively, are plotted as a function of the number of active users for three values of $\bar{\gamma}_b$. To maximize the $\mathrm{SINR_i}$ for each case at a given $\bar{\gamma}_b$, either γ_{opt} or $\varepsilon_{\mathrm{opt}}$ should be increased as the number of active users K increases.

The curves in Figs. 10 and 11 correspond to the same cases as illustrated in Figs. 5 and 6, respectively, except now the $\overline{\overline{\mathrm{SINR}}}_{(e)}$ is defined by (31), $\overline{\overline{\mathrm{SINR}}}_{(s)}$ is defined by (33), $P_e^{(e)} = Q(\sqrt{\max\lfloor \mathrm{SINR}_{(e)} \rfloor})$, and $P_e^{(s)} = Q(\sqrt{\max\lfloor \mathrm{SINR}_{(s)} \rfloor})$. Note that the y-axis of Fig. 10 is also not in decibels. Although the $\overline{\overline{\mathrm{SINR}}}$'s shown in Fig. 10 are not exactly the $\mathrm{SINR_i}$ for a specific user, it is a tradeoff measure for all users. The larger the processing gain N, the smaller the relative error between

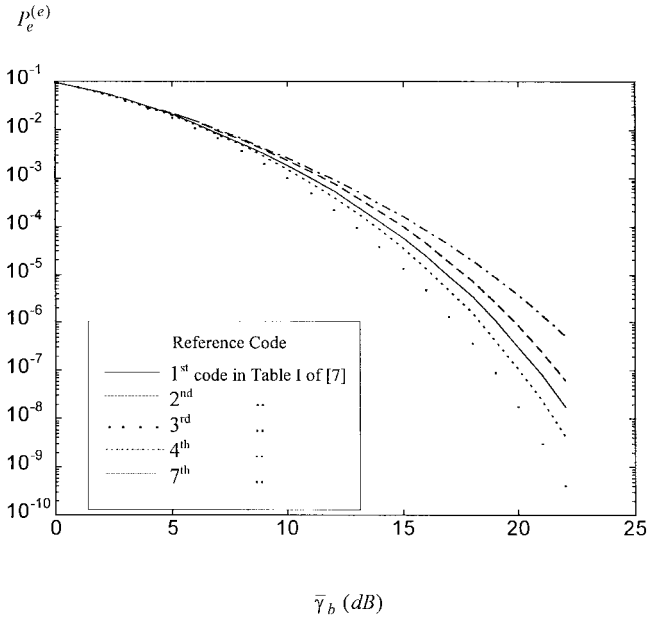

Fig. 8. Performance comparison of the proposed receiver for the EW case using different spreading codes when $N = 31$ and $K = 9$.

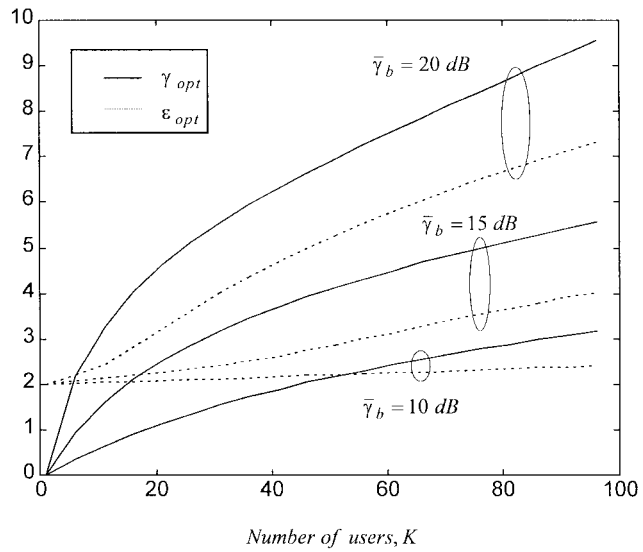

Fig. 9. The optimum parameters $\gamma_{\rm opt}$ and $\varepsilon_{\rm opt}$ versus the number of active users K for various values of $\bar{\gamma}_b$ when $N = 255$.

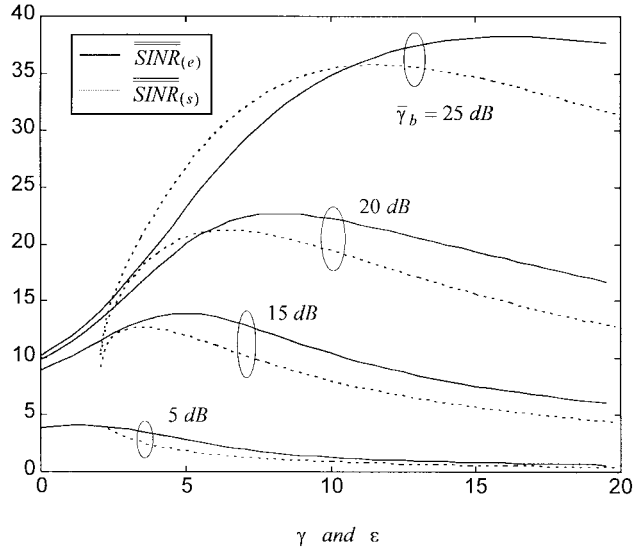

Fig. 10. $\overline{\overline{\rm SINR}}$ versus the parameters γ and ε for various values of $\bar{\gamma}_b$ when $N = 255$ and $K = 75$.

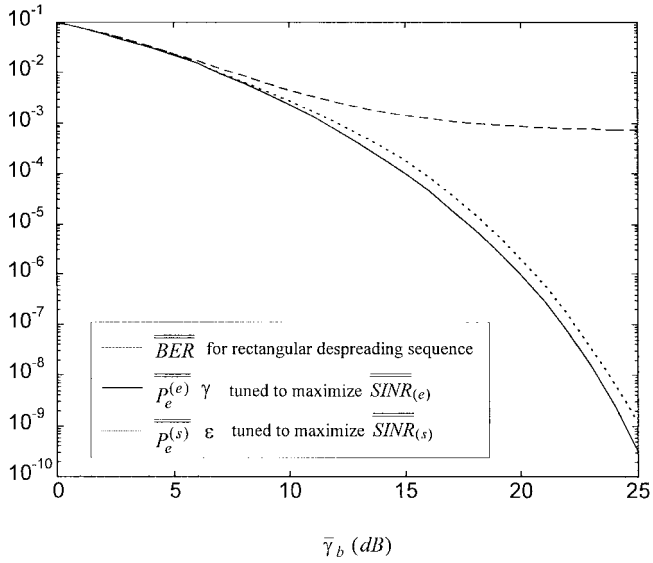

Fig. 11. $\bar{\bar{P}}_e$ versus $\bar{\gamma}_b$ for different WDS's when $N = 255$ and $K = 75$.

$\overline{\overline{\rm SINR}}$ and $\rm SINR_i$. When N is large, the main use of the curves in Fig. 10 would be to show roughly the values of both γ and ε, which maximize the corresponding system $\rm SINR_i$ for all user's code sequences. In Fig. 12, the parameters $\bar{\gamma}_{\rm opt}$ and $\bar{\varepsilon}_{\rm opt}$ which maximize the $\overline{\overline{\rm SINR}}_{(e)}$ and $\overline{\overline{\rm SINR}}_{(s)}$, respectively, are plotted as a function of the number of active users for three values of $\bar{\gamma}_b$.

V. Discussion

According to numerical results presented in the previous section, it is clear that the proposed receiver with WDS's outperforms the conventional receiver with rectangular despreading sequences. It can be argued that the results are optimistic due to the assumption of infinite bandwidth, and it is therefore important to see how the proposed system performs when the received signals are band-limited. As full analysis of the proposed system for band-limited signals is beyond the scope of this paper, we adopt a simple explanation to indicate the practical implication of the proposed system when the received signals are band-limited.

As is well known, a spreading signal with flat inband power spectral density (PSD) will yield, from the viewpoint of bandwidth efficiency, optimal performance in band-limited CDMA systems [7], [19], [14], [15], [17]. For example, in the IS-95 standard, each of the chip pulses of the transmitted signals is shaped approximately by a sinc function [18]. In this case, the inband spectrum of received spreading signals is already flat or nearly flat across a given bandwidth. It is not necessary to compensate for the spectrum at the receiver. There is, however, complicated steps in generating the transmit

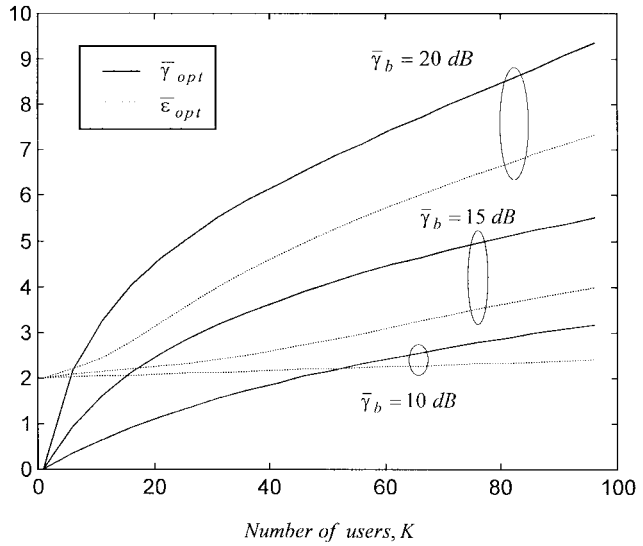

Fig. 12. The parameters $\bar{\gamma}_{\rm opt}$ and $\bar{\varepsilon}_{\rm opt}$ versus the number of active users K for various values of $\bar{\gamma}_b$ when $N = 255$.

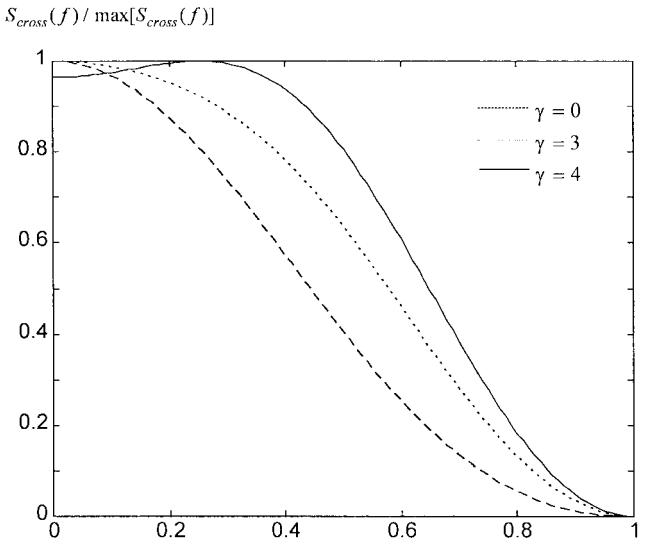

Fig. 13. Normalized cross PSD $S_{\rm cross}(f)/\max[S_{\rm cross}(f)]$ for three values of γ.

signals due to each pulse's long duration in the time-domain. In the proposed approach, band-limited spreading signals with nonflat spectrum pulses are transmitted. It is possible to design a variety of nonflat spectrum pulses [7]. Here, for simplicity, we only consider a system in which the baseband transmitted signal is generated by passing the spread signals through an analog low-pass filter with cutoff frequency at the first spectral null of the rectangular chip pulse. The resulting chip pulse is called main-lobe square-wave (MLSQ) pulse [7], [15]. A transmitter for such signals is very simple to implement. In this case, in order to achieve better performance, different techniques can be employed in the receiver to flatten the inband PSD of the received signals [14], [15]. As the outcome of the proposed approach is similar to a noise whitening technique, it must effectively whiten the inband PSD of the received signals. For illustration purposes, we consider only the EW case. Using results shown in [14], an appropriate measure of the performance for band-limited CDMA system is the cross power spectrum $S_{\rm cross}(f)$ of a pair of spreading and weighted despreading signals. To obtain $S_{\rm cross}(f)$, we first evaluate the cross-correlation function of $a_k(t)$ and $\hat{a}_k(t)$, defined by

$$R_{\rm cross}(t,\tau) \equiv E[a_k(t)\hat{a}_k(t-\tau)] \tag{39}$$

which depends on t as well as on τ. Assuming that the variable t in (39) is uniformly distributed on $[0, T_c]$ and then averaging (39) with respect to t, we obtain $R_{\rm cross}(\tau)$ which is independent of i. Thus $S_{\rm cross}(f)$ is the Fourier transform of $R_{\rm cross}(\tau)$ given by

$$\begin{aligned} S_{\rm cross}(f) = &\left(\frac{1}{T_c\omega^2(\gamma^2+\omega^2T_c^2)}\right) \\ &\cdot\Big\{2\omega^2T_c^2[1-\cos(\omega T_c)] + \gamma T_c\omega e^{-\gamma/2} \\ &\cdot[\sin(3T_c\omega/2) - 3\sin(T_c\omega/2)] \\ &+\gamma^2 e^{-\gamma/2}[\cos(T_c\omega/2) - \cos(3T_c\omega/2)]\Big\} \end{aligned} \tag{40}$$

where $\omega = 2\pi f$. When $\gamma = 0$, the chip weighting waveforms reduce to rectangular pulses, and $S_{\rm cross}(f)$ becomes

$$\lim_{\gamma\to 0} S_{\rm cross}(f) = \frac{2[1-\cos(\omega T_c)]}{\omega^2 T_c} \tag{41}$$

which is the auto PSD of the rectangular spreading signal. Assuming that the system bandwidth is constrained to satisfy $|f| \le 1/T_c$, Fig. 13 shows $S_{\rm cross}(f)$ versus the frequency f for three values of γ. From these curves, we can see that the inband portion of $S_{\rm cross}(f)$ can be flattened to a certain degree just by tuning γ in the receiver. This agrees with our intuitive interpretation, and we expect the performance of a band-limited CDMA system will be improved by using the proposed approach. It can be proved that the wider the bandwidth, the better the performance can be achieved by tuning γ, and when the system bandwidth extends to infinity, its performance is given by the previous sections.

For the purpose of comparison, Fig. 14 plots examples of the chip and spreading waveforms for the proposed and the IS-95 systems. In Fig. 14(a), solid and dashed curves are the MLSQ and the IS-95 chip waveforms, respectively. Each of the chip pulses is plotted by constraining its energy to T_c. In Fig. 14(b), the transmitted spreading signals of a length-14 segment with MLSQ chip pulses (solid line) and the IS-95 chip pulses (dashed line) are plotted. In the proposed approach, the waveform shown in Fig. 3(b) or (c) is used to despread the solid line signal in Fig. 14(b). Clearly, the spreading and despreading waveforms are quite different. For the IS-95 system, the despreading waveform should be the same as the spreading waveform [dashed line in Fig. 14(b)] for match filtering.

Finally, we mention issues relating to implementation. In a low chip rate system, we can simply use digital signal proces-

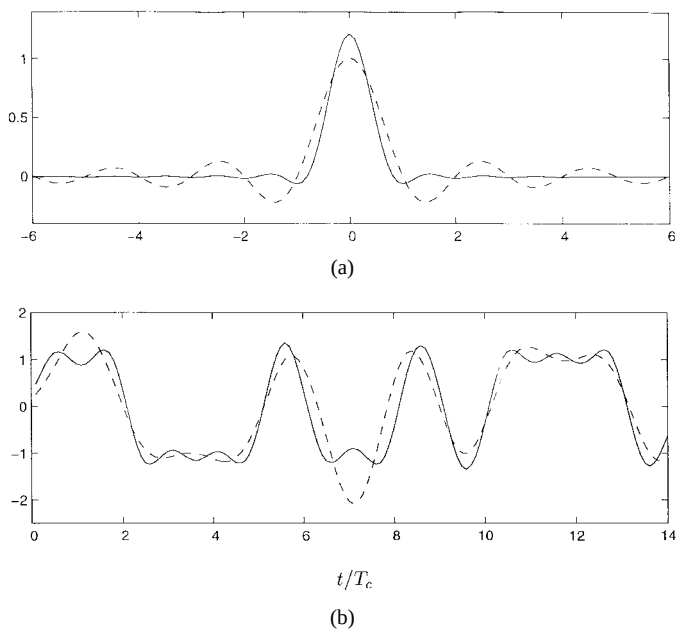

Fig. 14. Examples of chip and spreading waveforms for the proposed and the IS-95 systems: (a) MLSQ chip pulse (solid line) and the IS-95 chip pulse (dash line); (b) spreading waveforms for a length-14 segment with MLSQ chip pulses (solid line) and the IS-95 chip pulses (dash line).

sors to implement the WDS's. When the chip rate is high, the SW waveforms are preferred because they can be generated easily by using an analog switch controlled by digital logical circuits. Implementation of the proposed system appears to be much simpler, without making actual comparisons, than methods proposed in [15] to directly implement the optimum despreading function derived in [7].

VI. Conclusion

In this paper, we have presented an analysis of the performance of a DS-CDMA system using coherent receivers in which the despreading sequences are weighted by adjustable chip waveforms. The chip waveforms are designed with the objective of MAI rejection based on the concept that the despreading sequence emphasizes the transitions in the received spreading signal of interest. To maximize the system $\mathrm{SINR_i}$, we can simply tune the parameter γ or ε of the WDS under consideration based on the relative strength between the MAI and the AWGN. When the MAI is significant, receivers using the proposed adjustable despreading sequences outperform significantly receivers using fixed or rectangular despreading sequences. Numerical results show the despreading sequence weighted by EW performs marginally better than the SW. Finally, we have briefly analyzed the proposed system with band-limited spreading signals to reveal the practical implications.

Appendix A

In this appendix, the term $\mu_{ik|\{c_j^{(i)}\}}$ in (17) is examined. Letting $\tau_{ki} = qT_c - \tau_0$, where τ_0 is a random variable distributed uniformly on $[0, T_c]$ and q is an integer $\in [0, N-2]$, the expressions of $R_{ik}(\tau_{ki})$ and $\hat{R}_{ik}(\tau_{ki})$ can be written as

$$R_{ik}(\tau_{ki}) = \sum_{j_1=0}^{q} a_{N-1-q+j_1}^{(k)} f_{j_1}(\tau_0) + \sum_{j_1=0}^{q-1} a_{N-q+j_1}^{(k)} \hat{f}_{j_1}(\tau_0)$$
$$\hat{R}_{ik}(\tau_{ki}) = \sum_{j_2=q}^{N-1} a_{j_2-q}^{(k)} \hat{f}_{j_2}(\tau_0) + \sum_{j_2=q+1}^{N-1} a_{j_2-q-1}^{(k)} f_{j_2}(\tau_0) \tag{A-1}$$

where

$$f_p(\tau_0) = \int_0^{\tau_0} a_p^{(i)} w_p^{(i)}\left(t \,|\, \left\{c_p^{(i)}, c_{p+1}^{(i)}\right\}\right) dt$$
$$\hat{f}_p(\tau_0) = \int_{\tau_0}^{T_c} a_p^{(i)} w_p^{(i)}\left(t \,|\, \left\{c_p^{(i)}, c_{p+1}^{(i)}\right\}\right) dt. \tag{A-2}$$

By definition, we obtain

$$\begin{aligned}
&\mu_{ik|\{c_j^{(i)}\}} \\
&\quad = 2E[R_{ik}(\tau_{ki})\hat{R}_{ik}(\tau_{ki})] \\
&\quad = 2\sum_{j_1=0}^{q}\sum_{j_2=q}^{N-1} E\left[a_{N-1-q+j_1}^{(k)} a_{j_2-q}^{(k)} f_{j_1}(\tau_0)\hat{f}_{j_2}(\tau_0)\right] \\
&\qquad + 2\sum_{j_1=0}^{q}\sum_{j_2=q+1}^{N-1} E\left[a_{N-1-q+j_1}^{(k)} a_{j_2-q-1}^{(k)} f_{j_1}(\tau_0) f_{j_2}(\tau_0)\right] \\
&\qquad + 2\sum_{j_1=0}^{q-1}\sum_{j_2=q}^{N-1} E\left[a_{N-q+j_1}^{(k)} a_{j_2-q}^{(k)} \hat{f}_{j_1}(\tau_0)\hat{f}_{j_2}(\tau_0)\right] \\
&\qquad + 2\sum_{j_1=0}^{q-1}\sum_{j_2=q+1}^{N-1} E\left[a_{N-q+j_1}^{(k)} a_{j_2-q-1}^{(k)} \hat{f}_{j_1}(\tau_0) f_{j_2}(\tau_0)\right].
\end{aligned} \tag{A-3}$$

Note that $E[a_{r_1}^{(k)} a_{r_2}^{(k)}] = 0$ when $r_1 \neq r_2$. It is clear that the second, third, and fourth summing terms in (A-3) are zero. In the first summing term of (A-3), there is only one nonzero term which corresponds to the case where $j_1 = 0$ and $J_2 = N-1$. Therefore, we obtain

$$\begin{aligned}
\mu_{ik|\{c_j^{(i)}\}} &= 2E[f_0(\tau_0)\hat{f}_{N-1}(\tau_0)] \\
&= 2E\left[c_0^{(i)} \int_0^{\tau_0} w_0^{(i)}\left(t \,|\, \left\{c_0^{(i)}, c_1^{(i)}\right\}\right) dt \right. \\
&\qquad \left. \cdot \int_{\tau_0}^{T_c} w_{N-1}^{(i)}\left(t \,|\, \left\{c_{N-1}^{(i)}, c_0^{(i)}\right\}\right) dt\right]
\end{aligned} \tag{A-4}$$

which yields (22).

Appendix B

In this appendix, we evaluate the conditional variances of the MAI for both the EW and SW cases. Substituting (6) into (21) and then using (24), the conditional variance of MAI for the EW case, denoted by $\sigma^2_{IE|\{c_j^{(i)}\}}$, is approximately given by

$$\begin{aligned}
\sigma^2_{IE|\{c_j^{(i)}\}} &\approx P(K-1)\bar{\Theta}_{\{c_j^{(i)}\}}(R_{ik}, \hat{R}_{ik}) \\
&= \frac{NT_c^2(K-1)P}{\gamma^2} e^{-\gamma\Xi^{(e)}}\left(\Gamma^{\{c_j^{(i)}\}}, \gamma\right)
\end{aligned} \tag{B-1}$$

where (B-2) is defined, shown at the bottom of the next page. Similarly, substituting (7) into (21) and then using (24), the

conditional variance of MAI for the SW case, denoted by $\sigma^2_{IS|\{c_j^{(i)}\}}$, is approximately given by

$$\sigma^2_{IS|\{c_j^{(i)}\}} \approx \frac{N(K-1)}{\varepsilon^3} P T_c^2 \Xi^{(s)}\left(\Gamma^{\{c_j^{(i)}\}}, \varepsilon\right) \tag{B-3}$$

where (B-4) is defined, shown at the bottom of the page.

APPENDIX C

In this appendix, the ratios of $|E_{\{c_j^{(i)}\}}[\mu_{ik|\{c_j^{(i)}\}}]|$ to $E_{\{c_j^{(i)}\}}[\bar{\Theta}_{\{c_j^{(i)}\}}(R_{ik}, \hat{R}_{ik})]$ for the EW and SW cases, denoted by $\rho^{(e)}$ and $\rho^{(s)}$, respectively, are examined. Using (A-4), we obtain

$$\begin{aligned}\Pi &= E_{\{c_j^{(i)}\}}\left[\mu_{ik|\{c_j^{(i)}\}}\right] \\ &= \frac{1}{4}E[s_1\hat{s}_1 + s_1\hat{s}_3 + s_4\hat{s}_3 + s_4\hat{s}_1 - s_2\hat{s}_4 - s_2\hat{s}_2 \\ &\quad - s_3\hat{s}_2 - s_3\hat{s}_4]\end{aligned} \tag{C-1}$$

where

$$s_p = \int_0^{\tau_0} m_p(t)\,dt \quad \text{and} \quad \hat{s}_p = \int_{\tau_0}^{T_c} m_p(t)\,dt. \tag{C-2}$$

Note that τ_0 is a random variable distributed uniformly on $[0, T_c]$. For the EW and SW cases, the expression Π is denoted by $\Pi^{(e)}$ and $\Pi^{(s)}$, respectively. Substituting (6) and (7) into (C-1), we obtain

$$\begin{aligned}\Pi^{(e)} &= \Psi^{(e)}\left(-\frac{1}{2}+\frac{5}{2\gamma}-\frac{\gamma}{8}+\frac{7\gamma^2}{48}-\frac{\gamma e^{\gamma/2}}{8}\right. \\ &\quad \left.+2e^{\gamma/2}-\frac{4e^{\gamma/2}}{\gamma}+\frac{3e^{\gamma}}{2\gamma}-e^{\gamma}\right) \\ \Pi^{(s)} &= \Psi^{(s)}\left\{L^2(\varepsilon)\left(\frac{7}{6}+\varepsilon^2-2\varepsilon\right)+L(\varepsilon)(3\varepsilon-2-\varepsilon^2)\frac{5}{6}-\varepsilon\right\}\end{aligned} \tag{C-3}$$

where $\Psi^{(e)} = T_c^2 e^{-\gamma}/\gamma^2$ and $\Psi^{(s)} = T_c^2/\varepsilon^3$. For the EW case, since $\bar{\Theta}_{\{c_j^{(i)}\}}(R_{ik}, \hat{R}_{ik}) = \Psi^{(e)} N \Xi^{(e)}(\Gamma^{\{c_j^{(i)}\}}, \gamma)$ in (B-1), we obtain

$$\begin{aligned}E_{\{c_j^{(i)}\}}[\bar{\Theta}_{\{c_j^{(i)}\}}(R_{ik}, \hat{R}_{ik})] &= \Psi^{(e)} N E_{\{c_j^{(i)}\}}\left[\Xi^{(e)}\left(\Gamma^{\{c_j^{(i)}\}}, \gamma\right)\right] \\ &= \Psi^{(e)} N \bar{\Xi}^{(e)}(\gamma)\end{aligned} \tag{C-4}$$

where $\bar{\Xi}^{(e)}(\gamma)$ is given by (32). Similarly, for the SW case, since $\bar{\Theta}_{\{c_j^{(i)}\}}(R_{ik}, \hat{R}_{ik}) = \Psi^{(s)} N \Xi^{(s)}(\Gamma^{\{c_j^{(i)}\}}, \varepsilon)$ in (B-3), we obtain

$$\begin{aligned}E_{\{c_j^{(i)}\}}[\bar{\Theta}_{\{c_j^{(i)}\}}(R_{ik}, \hat{R}_{ik})] &= \Psi^{(s)} N E_{\{c_j^{(i)}\}}\left[\Xi^{(s)}\left(\Gamma^{\{c_j^{(i)}\}}, \varepsilon\right)\right] \\ &= \Psi^{(s)} N \bar{\Xi}^{(s)}(\varepsilon)\end{aligned} \tag{C-5}$$

where $\bar{\Xi}^{(s)}(\varepsilon)$ is given by (34). By definition, we obtain

$$\rho^{(e)} = \frac{|\Pi^{(e)}|}{\Psi^{(e)} N \bar{\Xi}^{(e)}(\gamma)} \quad \text{and} \quad \rho^{(s)} = \frac{|\Pi^{(s)}|}{\Psi^{(s)} N \bar{\Xi}^{(s)}(\gamma)} \tag{C-6}$$

yielding (36).

ACKNOWLEDGMENT

The authors wish to thank Dr. J. Wang and Dr. K. W. Yip for their valuable suggestions, and the anonymous reviewer who pointed out that a large computation effort is required in solving (3) when the spreading code has a period much larger than N.

$$\begin{aligned}\Xi^{(e)}\left(\Gamma^{\{c_j^{(i)}\}}, \gamma\right) &= \frac{1}{N}\left\{\Gamma^{(i)}_{\{-1,-1,-1\}}\left[4+\frac{12}{\gamma}-\frac{16}{\gamma}e^{\gamma/2}+\frac{4}{\gamma}e^{\gamma}\right]+\left(\Gamma^{(i)}_{\{-1,-1,1\}}+\Gamma^{(i)}_{\{1,-1,-1\}}\right)\right. \\ &\quad \cdot\left[\frac{5}{2}-\frac{\gamma}{4}+\frac{\gamma^2}{24}+\frac{19}{2\gamma}+e^{\gamma/2}-\frac{12}{\gamma}e^{\gamma/2}+\frac{5}{2\gamma}e^{\gamma}\right]+\left(\Gamma^{(i)}_{\{-1,1,1\}}+\Gamma^{(i)}_{\{1,1,-1\}}\right) \\ &\quad \cdot\left[-\frac{3}{2}-\frac{3}{4}\gamma+\frac{19}{24}\gamma^2-\frac{1}{2\gamma}+e^{\gamma/2}+\frac{e^{\gamma}}{2\gamma}\right]+\Gamma^{(i)}_{\{-1,1,-1\}}\left[-3-\frac{3}{2}\gamma+\frac{7}{12}\gamma^2-\frac{1}{\gamma}+2e^{\gamma/2}+\frac{e^{\gamma}}{\gamma}\right] \\ &\quad \left.+\Gamma^{(i)}_{\{1,-1,1\}}\left[1-\frac{\gamma}{2}+\frac{\gamma^2}{12}+\frac{7}{\gamma}+2e^{\gamma/2}-\frac{8}{\gamma}e^{\gamma/2}+\frac{e^{\gamma}}{\gamma}\right]+\gamma^2\Gamma^{(i)}_{\{1,1,1\}}\right\}\end{aligned} \tag{B-2}$$

$$\begin{aligned}\Xi^{(e)}\left(\Gamma^{\{c_j^{(i)}\}}, \varepsilon\right) &= \frac{1}{N}\left\{\Gamma^{(i)}_{\{-1,-1,-1\}}\left[\frac{8}{3}+4(\varepsilon-2)L(\varepsilon)+\frac{(\varepsilon-2)^2(4+\varepsilon)L^2(\varepsilon)}{3}\right]+\left(\Gamma^{(i)}_{\{-1,-1,1\}}+\Gamma^{(i)}_{\{1,-1,-1\}}\right)\right. \\ &\quad \cdot\left[\frac{5}{3}+\left(3\varepsilon-\frac{16}{3}\right)L(\varepsilon)+\left(\frac{\varepsilon^2}{3}-3\varepsilon+\frac{11}{3}\right)L^2(\varepsilon)\right]+\left(\Gamma^{(i)}_{\{-1,1,1\}}+\Gamma^{(i)}_{\{1,1,-1\}}\right) \\ &\quad \cdot\left[\frac{1}{3}+\left(\varepsilon-\frac{2}{3}\right)L(\varepsilon)+\left(\varepsilon^3-\varepsilon+\frac{1}{3}\right)L^2(\varepsilon)\right]+\Gamma^{(i)}_{\{-1,1,-1\}}\left[\frac{2}{3}+2\left(\varepsilon-\frac{2}{3}\right)L(\varepsilon)+\left(\varepsilon^3-2\varepsilon+\frac{2}{3}\right)L^2(\varepsilon)\right] \\ &\quad \left.+\Gamma^{(i)}_{\{1,-1,1\}}\left[\frac{2}{3}+\left(2\varepsilon-\frac{8}{3}\right)L(\varepsilon)+\left(\frac{\varepsilon^3}{3}-2\varepsilon+2\right)L^2(\varepsilon)\right]+\varepsilon^3L^2(\varepsilon)\Gamma^{(i)}_{\{1,1,1\}}\right\}\end{aligned} \tag{B-4}$$

REFERENCES

[1] S. Verdú, "Minimum probability of error for asynchronous Gaussian multiple-access channels," *IEEE Trans. Inform. Theory*, vol. IT-32, pp. 85–96, Jan. 1986.

[2] R. Lupas and S. Verdú, "Linear multiuser detectors for synchronous code-division multiple-access systems," *IEEE Trans. Inform. Theory*, vol. 35, pp. 123–136, Jan. 1989.

[3] Z. Xie, R. T. Short, and C. K. Rushforth, "A family of suboptimum detectors for coherent multiuser communications," *IEEE J. Select. Areas Commun.*, vol. 8, pp. 683–690, May 1990.

[4] M. K. Varanasi and B. Aazhang, "Near-optimum detection in synchronous code-division multiple-access systems," *IEEE Trans. Commun.*, vol. 39, pp. 725–736, May 1991.

[5] M. Varanasi and B. Aazhang, "Multistage detection in asynchronous code-division multiple access communications," *IEEE Trans. Commun.*, vol. 38, pp. 509–519, Apr. 1990.

[6] A. Duel-Hallen, "Decorrelating decision-feedback multiuser detector for synchronous code-division multiple access channels," *IEEE Trans. Commun.*, vol. 41, pp. 285–290, Feb. 1993.

[7] A. M. Monk, M. Davis, L. B. Milstein, and C. H. Helstrom, "A noise-whitening approach to multiple access noise rejection—Part I: Theory and background," *IEEE J. Select. Areas Commun.*, vol. 12, pp. 817–827, June 1994.

[8] E. A. Geraniotis and M. B. Pursley, "Performance of coherent direct sequence spread-spectrum communications over specular multipath fading channels," *IEEE Trans. Commun.*, vol. COM-33, pp. 502–508, June 1985.

[9] K. Yao, "Error probability of asynchronous spread spectrum multiple access communication systems," *IEEE Trans. Commun.*, vol. COM-25, pp. 803–809, Aug. 1977.

[10] J. S. Lehnert and M. B. Pursley, "Error probability for binary direct sequence spread-spectrum communications with random signature sequences," *IEEE Trans. Commun.*, vol. COM-35, pp. 87–98, Jan. 1987.

[11] N. M. Blachman and S. H. Mousavinezhad, "The spectrum of the square of a synchronous random pulse train," *IEEE Trans. Commun.*, vol. 38, pp. 13–17, Jan. 1990.

[12] A. D. Whalen, *Detection of Signals in Noise*. New York: Academic, 1971.

[13] M. B. Pursley, "Performance evaluation for phase-coded spread-spectrum multiple-access communication—Part I: System analysis," *IEEE Trans. Commun.*, vol. COM-25, pp. 795–799, Aug. 1977.

[14] L. Yu and J. E. Salt, "A hybrid spreading/despreading function with good SNR performance for band-limited DS-CDMA," *IEEE J. Select. Areas Commun.*, vol. 14, pp. 1576–1582, Oct. 1996.

[15] M. Davis, A. Monk, and L. B. Milstein, "A noise-whitening approach to multiple-access noise rejection—Part II: Implementation issues," *IEEE J. Select. Areas Commun.*, vol. 14, pp. 1488–1499, Oct. 1996.

[16] Y. C. Yoon and H. Leib, "Matched filters with interference suppression capabilities for DS-CDMA," *IEEE J. Select. Areas Commun.*, vol. 14, pp. 1510–1521, Oct. 1996.

[17] J. E. Salt and S. Kumar, "Effects of filtering on the performance of QPSK and MSK modulation in D-S spread spectrum systems using RAKE receivers," *IEEE J. Select. Areas Commun.*, vol. 12, pp. 707–715, May 1994.

[18] TIA/EIA, "Mobile station-base station compatibility standard for dual-mode wide-band spread spectrum cellular system," Tech. Rep. TIA/EIA/IS-95, July 1993.

Yuejin Huang (S'95–M'98), for a photograph and biography, see p. 1226 of the August 1999 issue of this TRANSACTIONS.

Tung-Sang Ng (S'74–M'78–SM'90), for a photograph and biography, see p. 1091 of the July 1999 issue of this TRANSACTIONS.